Compared Anatomy and Histology between *Mus musculus* Mice (Swiss) and *Rattus norvegicus* Rats (Wistar)

Giorgio Silva-Santana*[1,3,8], Fábio Aguiar-Alves[3], Licínio Esmeraldo da Silva[3,4], Maria Lúcia Barreto[5], Jemima Fuentes Ribeiro da Silva[6], Alexia Gonçalves[6], Ana Luíza Mattos-Guaraldi[1,7,8], Kátia Calvi Lenzi-Almeida[2,3]

[1] Institute of Microbiology Paulo de Góes, Federal University of Rio de Janeiro, Rio de Janeiro, Brazil.
[2] Environmental Science and Conservation Department, Medical College, Federal University of Rio de Janeiro, Rio de Janeiro, Brazil.
[3] Pathology Department, Medical College, Federal Fluminense University, Niterói, Rio de Janeiro, Brazil.
[4] Department of Statistics, Institute of Mathematics and Statistics, Federal Fluminense University, Niterói, Rio de Janeiro, Brazil.
[5] Centre for General Studies, Institute of Biology, Federal Fluminense University, Rio de Janeiro, Brazil.
[6] Histology and Embryology Department, Biomedical Center, University of the State of Rio de Janeiro, Rio de Janeiro, Brazil.
[7] Microbiology, Immunology and Parasitology Department, College of Medical Sciences, University of the State of Rio de Janeiro, Rio de Janeiro, Brazil.
[8] Laboratory of Diphtheria and Corynebacteria of Clinical Relevance, Faculty of Medical Sciences, University of the State of Rio de Janeiro, Rio de Janeiro, Brazil. The Collaborating Centre for Reference and Research on Diphtheria/National Health Foundation/Ministry of Health, Brazil

***Corresponding author**: Giorgio Silva de Santana. Universidade do Estado do Rio de Janeiro, Centro Biomédico. Avenida 28 de Setembro, nº 87 (Fundos) - 3º andar. Vila Isabel. CEP: 20551–030 - Rio de Janeiro, RJ – Brasil. Tel.: +55 (21) 28688280, Fax: +55 (21) 28688376; E-mail: bio.sant@hotmail.com

 doi:10.20944/preprints201907.0306.v1

Abstract

The evolution of knowledge in biological and medical areas which made possible scientific and technological advances are attributed to anatomical studies, physiology and immunology in animals, contributing to the discovery of prophylactic measures and treatments of diseases that affect humans and animals. Currently, substitution is suggested by alternative methods that do not use laboratory animals, however in vitro methods may never be able to provide similar results to in vivo methods. Mice and rats are the most used animals in experimental researches, the anatomical, histological and genetic differences between species should be carefully evaluated, to better apply the study model and avoid unnecessary waste avoid. This study, aimed at an anatomical comparative and histological relationship between a rat´s and a mouse´s organs, is of great importance in experimental studies. For such, 30 *Mus musculus* (Swiss) mice and 15 *Rattus norvegicus* (Wistar) male and heterogenic rats, were used. All animals were kept free of pathogenic microorganisms, with the absence of surgical interventions that could cause anatomical and physiological changes. It was possible to observe significant anatomical and histological differences between spleens, brains, hearts, stomachs and intestines, livers, eyes, lungs and kidneys among species, which will serve as a basis to assist in choosing the most satisfactory research model. Few studies relate specific characteristics among laboratory animals, being restricted to a few veterinary and zoology books. The greater the organic, physiological and anatomical similarities are with the human being, the greater is the applicability of the animals in studies. However, it is not possible to lay down general rules to validate the extrapolation from one species to another.

Keywords: anatomy, histology, mice, *Mus musculus*, rat, *Rattus norvegicus*.

 doi:10.20944/preprints201907.0306.v1

1. Introduction

The use of animals in a laboratory research for biological investigations was initially due to the relationship with the "study of comparative diseases" [1,2]. The objectives for these studies were to look for similarities in the origin and characteristics of the pathological processes that affected the human species, reproducing in animals found in the same conditions. Currently, the implantation of defined genetically and sanitarily laboratory animals has aided in new discoveries, through experimental models, contributing to the prevention of uncured diseases such as cancers, AIDS and multiple sclerosis, and also for the development of new surgical treatment techniques. Other applications correspond to the vaccines development, monoclonal antibodies, evaluation and control of biological products, pharmacology, toxicology, bacteriology, virology and parasitology and basic immunology studies, immunopathology, organ transplants and the immunosuppressive drugs development [3,4]. However, with technological advances, it is now possible to obtain satisfactory results through alternative methods in vitro, using cell culture and other methods, allowing the replacement of laboratory animals. However, animal models still have advantages, such as providing information about the body as a whole [5-8]. Although the close phylogenetic relationship or the anatomical conformity are factors that lead to the choice of the animal model, previous studies show that the extrapolation of results to humans cannot always be reliable [7,9-11].

Mice are the most used animals in experimental studies. The Asian species *Mus musculus*, was introduced as a laboratory animal in the XIX century. From this period on, it has also become an important experimental model for genetic studies [4,12]. It is common to use the Swiss albino lineage in scientific researches. Its easy acceptance and great use in experimental studies is due to the fact they are small, very prolific, short gestation period, easy domestication and maintenance [4,13]. Posteriorly, its use has become frequent, by genetic similarity of 99% with humans, allowing to establish mechanisms involved in human genetic disorders, and by the greater capacity of genetic modifications in up to 97% of the total of their genes [4].

In rats, the genre *Rattus* has 137 species, from the Central Asia regions. There are two species of great laboratory importance: *Rattus norvegicus* (domestic rat or brown rat) and the *Rattus rattus* (black rat) [14]. It is common to use in scientific researches the albino lineage Wistar species descendant from *Rattus norvegicus*, developed in Wistar Institute in Philadelphia in 1.906. This lineage was the first to be used as a model-organism at the time

 doi:10.20944/preprints201907.0306.v1

when researchers used primarily mice of the species *Mus musculus* [15]. Heterogenic animals have been used for various scientific purposes, as in researches correlated to rheumatology, endocrinology, orthopedics and others [16].

We consider them of great importance so that each laboratory knows the set of reference values of its healthy animals, according to the species, lineage, genre and age, to assist the professionals in their different studies. For this reason, the present study aims to address the general biology, anatomy and histology compared between organs of mice and rats used in the research.

2. Material and Methods

It was used data obtained from 30 *Mus musculus* (Swiss) mices heterogenic males, aged between 60 to 90 days, selected from control groups in a project approved by the Ethics Committee on Animal Use (CEUA) of the Pro-Rectory of Research, Post-Graduation and Innovation of the Fluminense Federal University (UFF), under the registration number: 439/2013. We also used data obtained from 15 *Rattus norvegicus* (Wistar) rats heterogenic males, aged between 90 to 120 days, selected from control groups in a project approved by the CEUA/UFF, under the registration number: 035/2011. All animals were from the Animal Core Laboratory (NAL/UFF), maintained in strict health control and free of specific pathogenic microorganisms (SPF). The animals were not submitted to any surgical intervention that could cause anatomical changes, nor were they exposed to any chemical or medicated treatment that could change its natural physiological state.

The mice were kept in collective cages in groups with five animals in bioterium of the Department of Pharmacy (UFF), the rats were kept in collective cages in groups containing three animals in bioterium of the Department of Nutrition and Dietetics (UFF). Both species received commercial ration Nuvilab® CR-1, containing in their composition the nutritional values required by the species, sterile water (autoclaved) *ad libitum*, kept in 12-hour light-dark cycles, with room temperature between 22°C (± 2°C) and humidity of 50%, according to recommendations by NAL/UFF.

2.2. Evaluation of absolute and relative weight

The absolute weight of the animals was measured using a precision scale (Marte - AD 2000, maximum load 210 g; sensitivity of 0.01 g).

Preprints (www.preprints.org) | NOT PEER-REVIEWED | Posted: 27 July 2019 doi:10.20944/preprints201907.0306.v1

The animals were euthanized with ketamine (150 mg/Kg) and xylazine (60 mg/Kg), after confirmation of cardiac and respiratory arrest, absence of corneal reflex and drop in body temperature < 25°C [17], were submitted the exsanguination by intracardiac puncture, for complete removal of blood in the cardiac chambers, which could lead to changes in the final values of the hearts' weights. Posteriorly, a necropsy was performed for the removal of organs: brain, heart, lungs, liver, spleen, kidneys, stomach, small intestine and large intestine. The eyes were extracted applying light pressure around the orbital cavity.

The organ weights were measured using a precision scale (Sartorius - BP 221S, maximum load 220 g; sensitivity of 0.1 mg). The pair organs, as the eyes, lungs and kidneys were weighed individually.

2.3. Evaluation of organ length and width

The organs were evaluated in relation to the anatomical form, coloring, length and width. Each organ was anatomically positioned to measure length and width using a titanium pachymeter (Mitutoyo - 6 inches, 150 mm) having as initial point the midline. Subsequently, they were photographed (photographic camera digital, Sony DSC-W310) and forwarded for anatomic-histological analysis.

2.4. Histology

The organs were sectioned symmetrically to the medium in the vertical orientation, positioned in cassettes, stored in formaldehyde at 10% with pH ~6-7 for 48h and submitted to the dehydration processes in growing concentrations of ethanol, diaphanization in xylol and inclusion in paraffin. Posteriorly, sections were made with thickness of 3 µm using microtome (LAB-MR500), having been the same fixed in blade and stained with hematoxylin and eosin (H&E). The slides were observed using optical microscope (model LX 500) and photographed using a camera iVm 5000 through the ProgRes program capture Pro 2.7 [18-20].

2.5. Statistical analysis

The variables of interest considered in the study were the absolute and relative body weights of two animal species and of its organs, the length and width of each organ. The data

 doi:10.20944/preprints201907.0306.v1

was statistically described by medium average and standard deviation. The correlation between the weights of pair organs with the same function as the eyes, lungs and kidneys, by means of Pearson correlation coefficient. Dispersion diagrams were used to allow visualization of the weights of the pair organs (lungs and kidneys) and included the expression of the regression straight and the coefficient of determination R^2 of the linear model. The comparison of body weights (absolute and relative), as well as organ weights between species was made by test t of Student (in independent or paired modality, when the data presented normality), or by the test of Mann-Whitney or of Wilcoxon/test of the sign (in the absence of normality). The length and width data comparison of each organ was made by using the correspondent weights tests. The investigation of the difference between numerical data variances of sets was carried out by Levene. The intervals of the confidence (I.C.) were presented to 95%. Statistical testing decisions, when not indicated instead, were sockets at the level of significance $p = 0.05$ (5%). The software PASW version 18.0 was used as a support for the statistical analyzes.

3. Results

3.1. Analysis among weight, length and width of the organ

The statistical description (mean ± standard deviation) of the weights, lengths and widths of the organs of rats and mice can be observed in tables 1 and 2. As expected, given the constitution animal physics, smaller measures occurred for the mice than for the rats, which was not always verified in the evaluation of the relative weights. The analysis of the relative weight of all organs revealed that there are statistically significant differences for mice and rats, in the following organs: heart, spleen, right and left kidney, right lung, liver and large intestine. However, there is no statistically significant evidence for left lung, brain, stomach and small intestine. From the significant differences, the relative weight of the mice´s organs exceeded the relative weight of the rat organs with greater expressiveness in the spleen, followed by the heart and other organs as right and left kidney, liver and large intestine with smaller expressiveness (Table 1).

In the pair organs correlation of the weights analysis with the same function, such as the lungs and kidneys, it was possible to observe in mice and rats a strong correlation (all larger than 0.800) (Figure 1). The relationship between lungs weights (right and left) of the Swiss mice presented a coefficient of Pearson correlation $r = 0.960$ ($p < 0.0001$) and of the r =

Preprints (www.preprints.org) | NOT PEER-REVIEWED | Posted: 27 July 2019 doi:10.20944/preprints201907.0306.v1

0.906 ($p < 0.0001$) between the weights of the kidneys (right and left). For Wistar rats, the observed correlations were r = 0.801 (value - $p = 0.0003$) and r = 0.857 ($p < 0.0001$), for the lungs and kidneys, respectively.

There was a statistically significant difference between the right lung weight and the weight of the left lung of Swiss mice (z = – 3.411; value - $p = 0.001$), with an average difference of 0.057 g and I.C. to 95% of the mean difference equal to [0.054; 0.060]. Regarding the weight of the right and left kidneys of the Swiss mice, a statistically significant difference was also observed (z = – 5.025; $p < 0.0001$), with mean difference of 0.056 g and I.C. to 95% for the mean difference of [0.051; 0.061]. For Wistar rats, right and left lungs and kidneys were statistically differentiated: lungs ($p < 0.0001$), with mean difference of 0.347 g and I.C. to 95% for the mean difference of [0.336; 0.361] and kidneys ($p < 0.0001$) with mean difference of 0.286 g and I.C. to 95% for the mean difference of [0.277; 0.296].

It was also observed that, in average, the right lung of mice is 71.32% heavier than the left lung and the right kidney is 28.26% heavier than the left kidney. In rats, similar data have been verified: in average, the right lung is 75.12% heavier than the left lung and the right kidney is 26.97% heavier than the left kidney.

In the comparative analysis between the weights of the organs of the two species, significant statistical differences were observed, as expected by its proportions, the values of the rats are superior to those of the mice. The 95% confidence intervals (I.C.) of the table 3 reinforce this fact.

3.2. Morphoanatomy and Histology

In mice the brain presents itself as lysencephalon. The brain can be divided into three anatomical parts: hindbrain (rhombencephalon), midbrain (mesencephalon) and forebrain (prosencephalon). The hindbrain connects the brain to the marrow spinal. The midbrain is situated between the hindbrain and the forebrain. The forebrain is composed by the cerebral cortex (telencephalon), higher trunk cerebral (diencephalon) and the olfactory bulb. In rats the brain presents sulcus, and it can be divided into telencephalon (cortex), diencephalon, midbrain, the bridge and, lastly, cerebellum and bulb. The brain tissue consists of functional cells (neurons) and the support cells: macroglia and microglia (Figure 2).

In both species, the eyes are paired with almost spherical shape. The inside out cornea consists of the outer layer of stratified squamous epithelium and of stroma formed by collagen fibers, fibroblasts, and some elastic fibers. The vitreous body fills the space between the lens

 doi:10.20944/preprints201907.0306.v1

(almost spherical and relatively large) and the retina. The lens consists of laminated fibers formed by modified epithelial cells, sealed per capsule. The retina is formed by retinal pigment epithelium, photoreceptor cell layer (containing mainly rods), outer nuclear layer (containing the receivers cell nuclei), outer plexiform layer, contains intermediate “bipolars”, “horizontals” and “amacrines” neurons which cross through the inner layer and the ganglion cell layer forming ganglion, where the cells form the axons of the optic nerve, leading the visual impulses to the brain. Lastly, the opaque sclera copper the posterior of the eyes (Figure 3).

The left lung is formed by one lobe, while the right lung is subdivided into cranial, middle, caudal and accessory. The lungs are formed by the bronchi that is divided into bronchioles and alveoli wrapped by capillaries. The arteries and veins follow the bronchial tree, the walls of the pulmonary veins contain heart muscle (striated) (Figure 4).

In mammals the heart has four chambers, two atria separated by an interatrial septum (IAS) and two ventricles separated by an interventricular septum (IVS). The heart consists almost exclusively of myocytes inside a fibrous leaf in stretch transversal marks (Figure 5).

The liver comprises four main lobes dorsally united. These are: large middle lobe (subdivided by a fissure in the left and right portion), right lateral lobe (divided horizontally into anterior and posterior portion), left lateral lobe and caudal lobe consisting of two portions in dorsally form of leaf and another ventrally to esophagus in the smallest stomach curve, its surface forms the papillary process. The blood is supplied to the liver through interlobular branches of hepatic arteries and hepatic veins that are open for the sinusoids. The vesicle biliary is located at the base of the profound bifurcation of the middle lobule next to the falciform ligament point of origin. The hepatocytes (parenchymal cells) are positioned on plates which radiate from the central vein to the lobular periphery (Figure 6).

The spleen has an elongated and triangular form in section transversal, with one postero-lateral face (diaphragmatic), one postero-medial face (renal), one antero-medial face (gastric) and one antero-lower face (colic). The splenic tissue is formed by parenchyma (splenic pulp) constituted by a differentiated cellular arrangement into a white pulp and red pulp. The white pulp presents a marginal zone lower cell density. Between the nodules we found the red pulp which constitutes the major part of the parenchyma (Figure 7).

The kidneys have the form of beans grain with a dark red coloration. The nephron is constituted by the glomerulus surrounded by Bowman's capsule. The parietal cells of Bowman's capsule are presented flattened in the vascular pole and cuboid on the glomerular urinary pole. The proximal tubules are found mainly in the cortex, formed by cuboidal cells

 doi:10.20944/preprints201907.0306.v1

with prominent brush border (microvilli). The distal tubules re-enter in the cortex and have a cuboid epithelium similar to that of proximal tubules but deprived of microvilli (Figure 8).

In rodents the stomach divides into aglandular and glandular, separated by margin pleated or limiting crest (*margo plicatus*). The aglandular portion is opaque with coloration whitish and coated by keratinized stratified pavement epithelium, while the glandular portion is translucent with reddish-pink coloration and coated with simple cubic epithelium. The mucosa of the glandular stomach can be divided into the cardiac region, located around the gastric opening of the esophagus extending to the edge of the pleated margin, containing mucous cells called "cardiac glands", the fundic region (ventral part of the stomach) is composed mainly by glandular mucosa containing "fundic glands" and granular eosinophilic parietal cells producing hydrochloric acid, lastly, the pyloric region extending to the pylorus (sphincter between the stomach and small intestine) contains pyloric mucous glands (Figure 9).

The intestine is slender and thick, having three layers during all its length (mucosa with submucosa, muscular and serous). In the mucosa epithelium of the small intestine there are scattered Paneth's cells, goblet cells and absorbent cells forming microvilli, which become smaller and in greater quantity from the duodenum toward to ileum (Figure 9). The large intestine is formed by the cecum, colon and rectum. The cecum has a corpuscle and apex, in their mice format is more elongated and any less saculad, and its mucosa forms transverse folds. The colon has an ascending part, one transverse and one descending part, the membrane of its mucosa contains goblet cells in greater proportion than in the small intestine, which form crypts with absence of villi (Figure 10).

4. Discussion

Surgical research using laboratory animals has expanded in recent decades as a result of a better anesthetic support, of sophistication in the infrastructure for monitoring during surgeries and of the incessant search for models that reproduce morbid conditions, in order to solve human diseases [21]. It´s important that the researcher knows the general biology, anatomy, histology and physiology of laboratory animals used in research, so he/she can choose the most appropriate experimental model. In the course of this work we can observe and compare some anatomical and histological features between *Mus musculus* and *Rattus norvegicus*.

 doi:10.20944/preprints201907.0306.v1

Different from rats, in mice the brain is lissencephaly (devoid in sulcus), the caudate nucleus and the putamen form a continuous structure (caudate putamen). Commonly, the brain of both species can be divided into three anatomical parts: rhombencephalon, midbrain and forebrain. The rhombencephalon connects the brain to the spinal cord (oblong) and is composed of marrow, pons (bridges) and cerebellum. The midbrain is located between the hindbrain and the prosencephalon, is constituted by tectum, integument and the cerebral peduncle. The forebrain is composed of the cerebral cortex (telencephalon), the basal ganglia, septum, epitalo, thalamus and hypothalamus (diencephalon or trunk cerebral higher) and the olfactory bulb. In the cerebral cortex, the right and left sides are connected by the corpus callosum, a thick band of nerve fibers [22,23].

The brain tissue consists of functional cells (neurons) and the support cells, macroglia and microglia. The macroglia are oligodendrocytes (central producer cells of myelin and astrocytes) present gray matter as well as white matter. The ependymal cells align the walls of the cerebral ventricles, are ciliated and may react positively with astrocytes. The epithelium of the choroid plexus form microvilli and reacts positively with epithelial markers [23,24].

In the mice´s brain, the rhombencephalon is responsible for muscle balance and control, and autonomous functions such as heart and respiratory rate [23,24]. The midbrain has structures responsible for receiving and interpreting visual and auditory signals [22-24]. In the hypothalamus are performed the endocrine functions and the survival instincts such as fight and flight and sexual. In the thalamus the sensory information is transmitted to the higher centers of the brain in the cortex [23,24]. The lumps and furrows in the cortex known as gyri and sulci, although they are abundant in the rat and other higher mammals, in mice there are few [23-25]. The genes responsible for the construction of the human brain and mice are 90% identical, therefore the use of these animals has great importance in studies of mental illness human [24].

The eyes are surrounded by structures that provide nutrition, protection and lubrication for the eyeball, including conjunctiva, eyelids, nictitating membrane (third eyelid), Harder gland and Meibomian glands [22-24]. The retina has peculiarities, absence of areas due to the night life mode, the visual acuity is increased by a central round area or "horizontal ray", it also does not have macula, under the light weak, the mouse pupil may have 1.2 mm diameter, in strong light contract about 0.2 mm diameter, in only half a second [24,26,27], can have two types of photoreceptors, which detect light and darkness (sticks) and one that detects colors (cones), but only two types of cones for green and blue colors. The blue cones are sensitive to lengths of shorter waves, so they can see in the ultraviolet [4,28]. It also has a neural grain

 doi:10.20944/preprints201907.0306.v1

"thick", each neural cell on the retina has a much bigger number of photoreceptors than humans, with an increase of sensitivity and reduction of acuity. Specifically, the ganglion rat receptive fields of cells are an order of greater magnitude than those of the human fovea [29]. Just presented in albino mice the "Bowman's membrane" has pigmentation as well as the retinal pigment epithelium [23,24].

The sclera of mice is opaque covering from the back to the eyes and the choroids with absence of tapetum lucidum [23-25]. In mice the ciliary body, iris and choroid form the external fibrous vascular tunica (uvea) containing pigment, except in albino species [23-25]. The lens consists of rolled fibers formed by modified epithelial cells, enclosed per capsule, allowed that almost all visible light and almost 50% of ultraviolet light exceed [23,30]. The ciliary muscle is poorly developed, making it impossible the change the form of the lens [26,31], unless it is dripped atropine, it can relax the lens keeping the focus, however, these facts are not conclusive [31,32]. Lastly, the nictitating membrane makes a translucent fold conjunctiva that together with the Harder's gland surround and protect the optic nerve [23,24].

The lungs are located in the thoracic cavity, covered by the parietal pleura. The left lung is compounded of a single lobe, while the right lung is subdivided in cranial, middle, caudal and accessory. However, there are described at least nine standards of pulmonary lobulation [23,24,33,34]. The main branch two bronchi form an intrapulmonary route with bifurcations ending in bronchioles. The smallest by air in the lungs of mice are the terminal bronchioles, that open for the alveolar ducts. The alveolar ducts take alveolar sacs and alveoli. The alveolar epithelium consists of lung cells type I and cuboidal cell type II. The lymphoid tissue (BALT associated with bronchial tissue) are few evident in the lungs of healthy mice, becoming well developed only in infections by pathogens [23,24,35]. The lungs receive blood of the systemic circulation, through of bronchial arteries and venous blood through the pulmonary arteries of the heart. The arteries and veins follow until the bronchial tree and on the walls of the pulmonary veins the cardiac muscles are present (striated) [23,24].

It was found significant difference between right and left lung weight, that is directly corelated to the number of lobules. In mice the right lung may be 71.32% heavier than the left and in rats this difference can come to 75.12%. Another important anatomic difference factor is the presence of the accessory lobe in rat and its absence in mice.

In mammals the heart has four chambers, two atria separated by an interatrial septum (IAS) and two ventricles separated by an interventricular septum (IVS) [22-24]. Between the IAS and IVS there is a small "septal segment" known as atrioventricular septum (AVS), result of the displacement of the atrioventricular valves (AV), placed between the subaortic segment

 doi:10.20944/preprints201907.0306.v1

about to leave of the left ventricle of the right atrium, being this structure relatively thick and mainly muscular [23,24]. At the junction in between the atria and ventricles (AVJ), there are two valves. On the left AVJ we found a mitral valve, that has two separate leaflets (bicuspid valve), while on the right AVJ a valve is found with three separate leaflets (tricuspid valve) [22-24]. The internal cover of the ventricles is characterized by the presence of numerous myocardial protrusions (trabeculae) [23,24]. Beyond trabeculation and chordae tendineae, inside of the apical cavity of the ventricles we can distinguish fine structures similar to tendon cords linked to the papillary muscle (trabeculae tendineae) [22-24].

The heart is constituted almost exclusively by myocytes specialized in the system of conduction (Purkinje cells) inside a fibrous leaf. The pulmonary veins join in confluence entering through single foramen on the dorsal wall of the left atrium [23,24].

The superiority between the relative weight of hearts of mice may be corelated with the arrangement of myocardial fibers, with greater quantity of myocardiocytes observed in histology. Another important factor that can contribute for these results is the heart rate from mice at rest (500 to 780 bpm) higher than the rats´ (250 to 480 bpm) [4,36,37].

The liver occupies one third of the anterior region of the abdominal cavity, its surface is covered by a capsule, formed by conjunctive tissue [23-25]. The blood flows from the perilobular region to the central vein, where is it conducted in large hepatic veins to the cava vein. The hepatocytes (parenchymal cells) are distributed on plates that radiate from the central vein to the lobular periphery, the sinusoidal coating cells (endothelial cells, Kupffer, fixed macrophages linked to cells of the wall of sinusoids and granular lymphocytes with natural killer activity - NK), have accumulation of cytoplasmic lipid and vitamin A, hematopoietic cells, cells of the bile duct, connective tissue cells and wall cells of blood vessels (adventitial cells and smooth muscle) [23,24]. A characteristic usually found in hepatic cells of rat and mice is anisocytosis and anisokaryosis (variations in size of cells and of your nuclei) [24].

The gallbladder is located in the base of deep division of the middle lobule next to the point of the origin of the falciform ligament [23,24,38]. Both the hepatic duct of the liver and the cystic duct of the gallbladder are united to form the common bile duct. This standard hepatic is the most common. There were described, however, at least 13 different patterns [33]. The gallbladder is observed only in mice, in rats the periportal biliary system is composed by a network of canaliculi that come together in a common bile duct [21].

The spleen is located in the left dorsocranial region of the abdominal cavity, posterior to the stomach and above of the upper pole of the left kidney. It has friable consistency and

 doi:10.20944/preprints201907.0306.v1

it's purple [22,23,39]. Both the color purple of greater intensity in the spleens of rats, and the superiority of the relative weight of the spleens of mice can be corelated to the venous sinuses (hematopoietic tissue), so in rats they are bigger and more abundant, making numerous anastamos (sinus) providing larger areas of red pulp, differently from the venous sinuses of the mice (non-ninsenics) [39]. Mice demonstrated to have greater proportion of white pulp than rats [39,40]. Finally, hematopoiesis extra medullary is common in the red pulp of rodents, with higher prevalence in the spleens of mice than of rats [39].

This body works as an immunological system and a blood reservoir of blood, it produces and matures B and T lymphocytes, making in some cases part of the reticuloendothelial system and participates of the hematopoiesis and hemocatheresis process (renovation of red blood cells) [39]. The red pulp is constituted reticular tissue with splenic cords (or Billroth) and venous sinuses (splenic sinuses) which go to the blood tissue (capillaries and sinusoids), in the leukocytes they are selected and destroyed if they present anomalies, are old or injured. Besides serving as a deposit of leukocytes and platelets, the macrophages contained therein are responsible for the phagocytosis of microorganisms [24,39,41]. The white flesh is subdivided in periarteriolar lymphoid sheath (PALS), follicles and marginal zone [41,42]. The internal PALS is composed predominantly by T CD4+ cells, T CD8+ cells in smaller number, dendritic cells and migrating B cells. The outer part is composed by small/medium lymphocytes (B and T cells) and macrophages, that after stimulation by an antigen can provide the storage of plasma cells. The follicles are continuations of the PALS, found in bifurcations of the central arterioles, compounds mainly by B lymphocytes, in smaller number by follicular dendritic cells and T CD4+ cells commonly T CD8+ cells are absent [39,43]. When stimulated by antigens, the follicles can form germinal centers with greater presence of follicular macrophages [39,40]. Lastly, the marginal zone is situated in the interface of red pulp with PALS and the follicles, is composed by reticular fibrils, macrophages of the marginal zone, dendritic cells and medium B cells [41,44]. The macrophages of the marginal zone are important in the removal of microorganisms and virus, recognition of receptors (TLRs) and recognition of bacteria [39,44], B cells have the phenotype IgM+/IgD contrary to follicular B cells with phenotype IgM+/IgD [39,43].

Kidneys are located parallel in the dorsal part of the abdominal cavity; the right kidney is lightly higher (cranially) than the left kidney [22-24]. The right kidney is usually bigger than the left one, and the kidneys of the males are relatively larger than the females´ [24]. This report justifies the fact of mice´s right kidney presents in mean 28.26% more weight than the

Preprints (www.preprints.org) | NOT PEER-REVIEWED | Posted: 27 July 2019 doi:10.20944/preprints201907.0306.v1

left one, similar results observed in the right kidney of rats, in mean 26.97% heavier than the left kidney.

In rats, the kidney is unilobar with a single papilla, formed by the cortex and medulla. In the cortex are found "cortical tubular labyrinths" (mainly proximal convoluted tubules) and "medullary rays" that extend from the medulla external [23]. The medulla is subdivided into outer zone with one "external and internal band" and the internal zone forms the papilla. The functional unit is the nephron, which consists of the glomerulus, wound in the proximal and distal tubule, in the descending and ascending portions of the Henle loop and in the straight portions [24]. The nephrons are connected to the collecting ducts, which outflow in the papillary ducts [22,23]. The papillary ducts open at the tip of the renal papilla in the renal pelvis [24]. The renal pelvis is coated with transitional cell epithelium and its continuation forms the ureter [22]. The renal papilla in rats can be long and projects in the initial portion of the ureter [23]. The glomerulus is surrounded by Bowman's capsule, most rat's species may exhibit sexual dimorphism under the influence of testosterone (the parietal epithelial cells are presented in the males and flattened in females) [22,24].

Regardless of the genus, the parietal cells of Bowman's capsule are presented flattened in the vascular pole and cuboidal in the urinary pole of the glomeruli [23,24]. The proximal tubules are found mainly in the cortex, composed of cuboidal cells with brush border prominent (microvilli) [22,23]. The descending and ascending portions of the Henle loop are found in the marrow, coated with flattened epithelium that resembles to the endothelium of blood vessels [24]. The distal tubules re-enter the cortex and have a cuboidal epithelium similar to that of proximal tubules, but devoid of a brush border [22]. The straight portion of the distal tubules leads to dense macula in the vascular pole of the glomerulus, where renin is produced by specialized cells [24]. In rats the renal vasculature resembles other species, the branches of the renal artery fashion the arcuate arteries on the corticomedullar border [23]. The interlobular branches of the arteries arched suprem the afferent arterioles of the glomeruli [22,24]. The efferent arterioles provide blood to the cortex and form the downward straight vessel which supplies blood to the marrow [23,24]. Venous blood is collected in the ascending vessel and in the arched interlobular veins spontaneously occurring vacuolation, probably of lysosomal origin, in the renal tubular epithelium of the medulla external [22,23].

In rodents the stomach is divided into glandular and non-glandular parts [24,38,45]. The non-glandular stomach usually has thin and transparent walls, coated by epithelium stratified keratinized squamous, serving for storage and food digestion. The glandular stomach has thick walls coated by epithelium, the blade itself is occupied by tubular gastric

 doi:10.20944/preprints201907.0306.v1

glands containing cells which secrete mucus and pepsinogen, main cells and parietal cells secretory of hydrochloric acid (HCl) [21,23,24,45]. The initial portion of duodenum is equipped with special alveolar tubule glands called "Brunner glands" [23,24]. One or more pancreatic ducts and the common bile duct are open in duodenal papilla [24]. The use of models that replicate ulcer disease should consider the installation of ulcers in non-secretory mucosa, studies with this objective should be evaluated very rigorously, because it is not easy to produce ulcer in the gastric mucosa of rats, and most of the suggested methods for the origin of ulcer disease frequently submit the animal to suffering [21].

The intestine is divided into thin and thick, during the entire length there are three layers (mucosa with submucosa, muscular and serous) [23,24,38]. The mucosa has lining epithelium and fibrovascular stroma called "own blade", which is separated from the submucosa by "mucosal muscular lamina" (a thin layer of smooth muscle) [23,24]. The submucosa is formed by connective tissue involving blood vessels, lymphatic vessels and nerves. The muscle consists of the inner circular layer of muscle. The serosa is formed by the thin layer of peritoneum [23,24,38].

In the intestine the lymphoid tissue (GALT) forms scattered nodules the submucosa and lamina propria. The aggregates larger fashion "Peyer's patches", which in the small intestine are located in front of mesenteric accessory, on surface of epithelium of the "antimesenteric" portion are the "M cells" that work as presenters of antigen [45]. In the large intestine the "Peyer's patches" are not strictly antimesenteric. The mucosal epithelium commonly has absorptive cells, with membrane luminal cell forming microvilli, a greater amount of goblet cells than in small intestine forming crypts. The Paneth's cells are especially great on rat, containing eosinophils (granulocytes) with lysozyme and peptides antimicrobial. The enteroendocrine cells polypeptide and are distributed diffusely along the gastrointestinal tract. The cells "caveolae" are responsible for the production of intestinal chemoreceptors [23,24]. In entrance of ileum form itself the "sacculus rotundus" and exit of the colon form the "ampulla coli" [24].

In rats the mucosal surface of small intestine has no folds (plicae) that are found in greater species. The mucosa forms villi of epithelium and lamina propria, designing the inner intestinal lumen [23,24,38], decreasing villi from the duodenum towards the ileum, every single one contains one lymphatic vessel (lacteal) [23,24]. Between the villi there are protrusions in the opposite direction, under the surface of mucosa forming "crypts" or "intestinal glands" [23,24,38].

In mice and rats the cecum is functional, has large size with sacculations, forming a "fermentation tank" where specialized microorganisms degrade cell walls formed by cellulose, in rats the cecum has a corpuscle and apex, its mucosa forms transverse folds [45]. The colon has an ascending part, a transverse part and a descending part. The mucosa has an ascending and transverse part forming transverse folds, in the descending colon and in rectum there are longitudinal protuberances prominent in the lumen, formed by the mucosa and submucosa. The muscular mucosa is more prominent in rectum than in colon and in the transition from rectum for anus, the superficial epithelium becomes squamous stratified, around the anus presenting sebaceous modified glands ("circum-anal gland") [23,24,38].

5. Conclusion

Few are the studies which correlate specific characteristics between animal species used in researches, except a few veterinary and zoology books. Today we can dispose of experimental more refined models, maintaining and intensifying phenotypic characteristics and specific genotypic, since its genome is a result of directed mating. It is known that the greater similarity between the physiological, anatomical and organic characteristics with human, the greater applicability of animals in studies and the reliability of results. However, it is not possible to establish reliable general rules to validate extrapolation from one species to another.

Mice and rats are the most used species in researches, for being better known scientifically and by the advantages over other species, such as smaller physical size and higher weight, easy locomotion and lower financial cost for maintenance. Currently, there are multiple lineages of mice and rats available destined to different objectives of studies. However, studies using animals require from the researcher careful planning, knowledge of laws and country´s guidelines, ethical principles and, above all, be up to date on previous researches in the same area, so they can avoid repetition of tests and inconclusive results acquisition which would lead to waste, enabling the choice of the most suitable species.

Currently, with technological advances, alternative methods are being developed, as in vitro studies. However, the models that use animals, still have the advantage obtaining information about the organism as a whole.

Acknowledgements: We would like to thank Pathology Program/UFF, Institute of Microbiology Paulo de Góes/UFRJ, Laboratory of Diphtheria and Corynebacteria of Clinical

Relevance/UERJ. This study was financed in part by the National Council for Scientific and Technological Development (CNPq), Coordination for the Improvement of Higher Level Personnel - Brazil (CAPES) - Finance Code 001 and Research Support Foundation for the State of Rio de Janeiro - Brazil (FAPERJ).

Disclosure of potential conflicts of interest: The authors declare no conflict of interest.

Ethics Approval: All experimental protocols were approved by the Ethical Committee for Animal Research of Fluminense Federal University.

Referências

[1] Feijó, A.G.S.; Braga, L.M.G.M.; Pitrez, P.M.C. Animais na pesquisa e no ensino: aspectos éticos e técnicos. Porto Alegre: EdiPUCRS. 2010; pp. 421.

[2] Neves, S.M.P. Manual de cuidados e procedimentos com animais de laboratório do Biotério de Produção e Experimentação da FCF-IQ/USP. São Paulo. 2013; pp. 216.

[3] Andrade, A.; Pinto, S.C.; Oliveira, R.S. orgs. Animais de laboratório: criação e experimentação [online]. Rio de Janeiro: Ed. Fiocruz. 2002; pp. 388. ISBN: 85-7541-015-6. Available from: SciELO Books.

[4] Chorilli, M.; Michelin, D.C.; Salgado, H.R.N. Animais de laboratório: o camundongo. *Rev Ciênc Farm Básica Apl*. **2007**, 28, 11-23.

[5] Heywood, R. The use of animals in testing. *ATLA*. **1987**, 329-333.

[6] Ribeiro, S.M.L.; Campos, P.; Tirapegui, J. Rat as an experimental animal: history, biological data and critical analysis of its usage. *Rev Farm Bioquím Univ São Paulo*. **1995,** 31, 21-28.

[7] Salén, J.C.W. Animal models: principles and problems. In: Rollin, B.E.; Kessel, M.L. editors. The experimental animal in biomedical research: care, husbandry and well-being: an overview by species. 3ª ed. Boston: CRC Press. 1995; pp. 560.

[8] Snitkoff, G.G. Testes biológicos. In: Gennaro AR. Remington: a ciência e a prática da farmácia. 20ª ed. Rio de Janeiro: Guanabara Koogan. 2004; pp. 556-568.

[9] Calabrese, E.J. Principles of animal extrapolation. Michigan: Ed. Lewis Publishers. 1991.

[10] Lynette, A.H. Responsible conduct with animals in research. 1ª ed. England: Oxford University. (October 8, 1998). 1998.

[11] Fagundes, D.J.; Taha, M.O. Animal disease model: choice´s criteria and current animals specimens. *Acta Cir Bras.* **2004**, 19, 59-65.

[12] Santos, B.F. Camundongos mutantes mais utilizados. In: Andrade, A.; Pinto, S.C.; Oliveira, R.S. Animais de laboratório: criação e experimentação. Rio de Janeiro: Fiocruz. 2002a; pp. 139-142.

[13] Santos, B.F. Criação e manejo de camundongos. In: Andrade, A.; Pinto, S.C.; Oliveira, R.S. Animais de laboratório: criação e experimentação. Rio de Janeiro: Fiocruz. 2002b; pp. 115-118.

[14] Cesarino, J.L.; Gontijo, J.A.R.; Zapparoli, A. Environment in an experimental animal facility and the species *Rattus norvegicus*: review. *Rev Eletr Farm*. **2011**, 8, 25-32.

[15] Clause, B.T. The Wistar Institute Archives: rats (not mice) and history. *Mendel News*. **1998**; 7, 2-7.

[16] Andersen, M.L.; D´Almeida, V.; Ko, G.M. et al. Eutanásia. In: Andersen, M.L.; D´Almeida, V.; Ko, G.M.; Kawakami, R.; Martins, P.J.F. Princípios éticos e práticos do uso de animais de experimentação. São Paulo: UNIFESP - Universidade Federal de São Paulo. 2004; pp. 71-79.

[17] Lima, J.B.A.; Skare, T.L.; Malafaia, O. et al. Sepsis inducing syndrome of multiple organ dysfunction: an experimental study in rats. *ABCD Arq Bras Cir Dig*. **2011**; 24, 95-102.

611 [18] Silva-Santana, G.; Lenzi-Almeida, K.C.; Fernandes-Santos, C. et al. Mice infection by
612 methicillin-resistant *Staphylococcus aureus* from different colonization sites in humans
613 resulting in difusion to multiple organs. *J Clin Exp Pathol*. **2016**; 6, 1000283.
614
615 [19] Silva-Santana, G.; Lenzi-Almeida, K.C.; Lopes, V.G.S. et al. Biofilm formation in
616 catheter-related infections by Panton-Valentine leukocidin-producing *Staphylococcus aureus*.
617 *Int Microbiol*. **2016**; 19, 199-207.
618
619 [20] Silva-Santana, G.; Lenzi-Almeida, K.C.; Lopes, V.G.S. et al. Atypical manifestation in
620 infection by methicillin-resistant *Staphylococcus aureus* carrier SCC*mec* IV and Panton-
621 Valentine Leukocidin-producer in experimental sepsis model. *Afr J Microbiol Res*. **2017**; 11,
622 724-728.
623
624 [21] Schanaider, A.; Silva, P.C. The use of animals in experimental surgery. *Acta Cir Bras*.
625 **2004**; 19, 441-447.
626
627 [22] Morawietz, G.; Ruehl-Fehlert, C.; Kittel, B. et al. Revised guides for organ sampling and
628 trimming in rats and mice. *Exp Toxic Pathol*. **2004**; 55, 433-449.
629
630 [23] Treuting, P.M.; Dintzis, S.M.; Liggitt, D. et al. Comparative anatomy and histology: a
631 mouse and human atlas. Elsevier. 2012; pp. 457.
632
633 [24] Krinke, G.J. Normative histology of organs. The laboratory mouse. 21st. 2004; 9, pp.
634 133-166.
635
636 [25] Cook, M.J. The anatomy of the laboratory mouse. Elsevier. 1965; pp. 143.
637
638 [26] Lashley, K.S. Studies of cerebral function in learning. VIII. A reanalysis of data on mass
639 action in the visual cortex. *J Comp Neurol*. **1932**; 54, 77-84.
640
641 [27] Remtulia, S.; Hallett, P. A schematic eye for the mouse, and comparisons with the rat.
642 *Vision Res*. **1985**; 25, 21-31.
643

644 [28] Jacob, L.; Beecken, V.; Bartunik, L.J. et al. Purification and crystallization of yeast
645 hexokinase isoenzymes. Characterization of different forms by chromatofocusing. *J*
646 *Chromatogr*. **1991**; 587, 85-92.
647
648 [29] Brown, J.E.; Rojas, J.A. Rat retinal ganglion cells: receptive field organization and
649 maintained activity. *J Neurophysiol*. **1965**; 28, 1073-1090.
650
651 [30] Gorgels, T.G.; van Norren, D. Spectral transmittance of the rat lens. *Vision Res*. **1992**;
652 32, 1509-1512.
653
654 [31] Woolf, D. A comparative cytological study of the ciliary muscle. *Anat Rec*. **1956**; 124,
655 145-163.
656
657 [32] Artal, P.; Tejada, P.H.; Tedó, C.M. et al. Retinal image quality in the rodent eye. *Vis*
658 *Neurosci*. **1998**; 15, 597-605.
659
660 [33] Hummel, K.P.; Richardson, E.L.; Fekete, E. Anatomy. In: Biology of the laboratory
661 mouse, 2ª ed. (editors Green, E.L.; Fahey, E.U.), 1975; pp. 247-307. Dover Publications, New
662 York.
663
664 [34] Kittel, B.; Ruehl-Fehlert, C.; Morawietz, G. et al. Revised guides for organ sampling and
665 trimming in rats and mice. *Exp Toxic Pathol*. **2004**; 55, 413-431.
666
667 [35] Souza, J.B.; Oliveira, M.T.; Nascimento, E.R. et al. *Mycoplasma pulmonis*, murine
668 respiratory mycoplasmosis agent: review. *Arch Vet Sci*. **2016**; 21, 08-25.
669
670 [36] Ko, G.M.; DeLuca, R.R. Camundongo. In Lapchik, V.; Mattaraia, V.; Ko, G. (editors)
671 Cuidados e manejos de animais de laboratório. 1ª ed. São Paulo: Editora Ateneu. 2009; pp.
672 137-167.
673
674 [37] Oliveira, F.S.; Range, J.A.; Batista, W.S. et al. Influence of paternal aggression in the
675 physical/emotional development of swiss Webster mice in laboratory environment.
676 *RESBCAL*. **2014**; 2, 244-253.
677

678 [38] Ruehl-Fehlert, C.; Kittel, B.; Morawietz, G. et al. Revised guides for organ sampling and
679 trimming in rats and mice. *Exp Toxic Pathol*. **2003**; 55, 91-106.
680
681 [39] Cesta, M.F. Normal structure, function, and histology of the spleen. *Toxicol Pathol*.
682 **2006**; 34, 455-465.
683
684 [40] Ward, J.M.; Mann, P.C.; Morishima, H. et al. Thymus, spleen, and lymph nodes. In:
685 Pathology of the mouse (editors Maronpot, R.R.), 1999; pp. 333-60. Cache River Press,
686 Vienna, Illinois.
687
688 [41] Veerman, A.J.P.; van Ewijk, W. White pulp compartments in the spleen of rats and mice.
689 A light and electron microscopic study of lymphoid and non-lymphoid cell types in T-and B-
690 areas. *Cell Tiss Res*. **1975**; 156, 417-441.
691
692 [42] Saito, H.; Yokoi, Y.; Watanabe, S. et al. Reticular meshwork of the spleen in rats studied
693 by electron microscopy. *Am J Anat*. **1988**; 181, 235-52.
694
695 [43] van Rees, E.P.; Sminia, T.; Dijkstra, C.D. Structure and development of the lymphoid
696 organs. In: Pathobiology of the aging mouse (editors Mohr, U.; Dungworth, D.L.; Capen,
697 C.C.; Carlton, W.W.; Sundberg, J.P.; Ward, J.M.), 1996; 1, 173-187. ILSI Press, Washington,
698 D.C.
699
700 [44] Mebius, R.E.; Kraal, G. Structure and function of the spleen. *Nat Rev Immunol*. **2005**; 5,
701 606-616.
702
703 [45] Kararli, T.T. Comparison of the gastrointestinal anatomy, physiology, and biochemistry
704 of humans and commonly used laboratory animals. *Biopharm Drug Dispos*, **1995**; 16, 351-
705 380.
706
707
708
709
710
711

Preprints (www.preprints.org) | NOT PEER-REVIEWED | Posted: 27 July 2019 doi:10.20944/preprints201907.0306.v1

Table 1. Absolute and relative weight values.

Organs	Species	Absolute weight	Comparison of species		Relative weight	Comparison of species	
		mean ± standard deviation	statistical test	value-*p*	mean ± standard deviation	statistical test	value-*p*
Body (weight total)	Mice Rat	34.001 ± 1.3031 189.39 ± 1.7142	t de Student t = 346.367; gl = 46	< 0.0001 (*)			
Brain	Mice Rat	0.4415 ± 0.05969 2.7061 ± 0.05916	Mann-Whitney U = 0	< 0.0001 (*)	0.0130 ± 0.00143 0.0143 ± 0.00021	Mann-Whitney U = 142	0.116
Eyes	Mice Rat	0.0224 ± 0.00083 0.1328 ± 0.00811	Mann-Whitney U = 0	< 0.0001 (*)	0.0007 ± 0.00002 0.0007 ± 0.00004	Mann-Whitney U = 71	0.0003 (*)
Left lung	Mice Rat	0.0801 ± 0.01062 0.4641 ± 0.03702	Mann-Whitney U = 0	< 0.0001 (*)	0.0024 ± 0.00026 0.0024 ± 0.00018	Mann-Whitney U = 179.5	0.133
Right lung	Mice Rat	0.1372 ± 0.01833 0.8127 ± 0.03368	t de Student t = – 74.362; gl = 17.115	< 0.0001 (*)	0.0040 ± 0.00042 0.0043 ± 0.00014	t de Student t = – 5.566; gl = 38.725	< 0.0001 (*)
Heart	Mice Rat	0.1443 ± 0.01734 0.7203 ± 0.01118	Mann-Whitney U = 0	< 0.0001 (*)	0.0042 ± 0.00040 0.0038 ± 0.00004	Mann-Whitney U = 81	0.0001 (*)
Liver	Mice Rat	2.0446 ± 0.02832 11.3733 ± 0.02776	Mann-Whitney U = 0	< 0.0001 (*)	0.0606 ± 0.00176 0.0601 ± 0.00042	Mann-Whitney U = 106	0.011 (**)
Spleen	Mice Rat	0.1204 ± 0.02476 0.4366 ± 0.01833	t de Student t = – 51.978; gl = 40	< 0.0001 (*)	0.0035 ± 0.00063 0.0023 ± 0.00008	t de Student t = 10.371; gl = 28.257	< 0.0001 (*)
Left kidney	Mice Rat	0.1982 ± 0.00746 1.0616 ± 0.01314	t de Student t = – 244.004; gl = 16.679	< 0.0001 (*)	0.0058 ± 0.00014 0.0056 ± 0.00005	Mann-Whitney U = 28	< 0.0001 (*)
Right Kidney	Mice Rat	0.2542 ± 0.01965 1.3479 ± 0.02656	Mann-Whitney U = 0	< 0.0001 (*)	0.0075 ± 0.00047 0.0071 ± 0.00010	Mann-Whitney U = 73.5	< 0.0001 (*)
Stomach	Mice Rat	0.2823 ± 0.01160 1.5855 ± 0.01120	Mann-Whitney U = 0	< 0.0001 (*)	0.0084 ± 0.00022 0.0084 ± 0.00005	Mann-Whitney U = 178.5	0.537
Small intestine	Mice Rat	1.5073 ± 0.01160 8.3373 ± 0.01118	Mann-Whitney U = 0	< 0.0001 (*)	0.0402 ± 0.01370 0.0440 ± 0.00036	Mann-Whitney U = 151	0.077
Large intestine	Mice Rat	0.8676 ± 0.01196 4.8105 ± 0.01153	Mann-Whitney U = 0	< 0.0001 (*)	0.0257 ± 0.00074 0.0254 ± 0.00019	Mann-Whitney U = 101.5	0.007 (*)

(*) $p < 0.01$; (**) $p < 0.05$.

Preprints (www.preprints.org) | NOT PEER-REVIEWED | Posted: 27 July 2019 doi:10.20944/preprints201907.0306.v1

Table 2. Length and width values.

Organs	Species	Length (mm)	Width (mm)
		mean ± standard deviation	mean ± standard deviation
Brain	Mice	13.52 ± 0.54	12.49 ± 0.44
	Rat	23.63 ± 0.63	16.73 ± 0.45
Eyes	Mice	3.5 ± 0 (constant radius)	
	Rat	7.0 ± 0 (constant radius)	
Left lung	Mice	11.26 ± 0.56	5.22 ± 0.35
	Rat	23.04 ± 1.64	10.67 ± 1.79
Right lung	Mice	13.45 ± 1.19	6.16 ± 0.28
	Rat	26.09 ± 1.82	12.04 ± 0.43
Heart	Mice	8.08 ± 0.2	6 ± 0.11
	Rat	12.54 ± 0.4	10.01 ± 0.1
Liver	Mice	28.66 ± 0.98	24.46 ± 5.17
	Rat	37.37 ± 1.27	42.03 ± 1.03
Spleen	Mice	15.2 ± 0.7	4.64 ± 0.41
	Rat	31.89 ± 1.32	6.77 ± 0.39
Left kidney	Mice	10.79 ± 0.83	6.28 ± 0.42
	Rat	15.65 ± 2.07	8.57 ± 0.33
Right kidney	Mice	10.74 ± 0.66	6.1 ± 0.43
	Rat	16.92 ± 0.97	9.1 ± 0.57
Stomach	Mice	13.02 ± 1.12	5.72 ± 1.01
	Rat	25.69 ± 1.32	13.23 ± 1.02
Small intestine	Mice	371.99 ± 1.07	1.87 ± 0.61
	Rat	506.06 ± 0.85	5.09 ± 1.03
Large intestine	Mice	116.02 ± 1.12	2.88 ± 0.91
	Rat	222.46 ± 1.32	8.09 ± 1.03

 doi:10.20944/preprints201907.0306.v1

Table 3. Comparison between weights of the organs of mice and rats.

Organs	Species	Middle-weight (g)	Analysis of the homogeneity of variances (test of Levene)		Average weight difference (g)	Standard weight difference error (g)	Comparison between organ weights between mice and mice			I.C. at 95% for the difference between the weights of animals' organs
			statistic f	value-*p*			statistic t	g.l.	value-*p*	
Brain	Mice Rat	0.442 2.706	0.313	0.579	2.265	0.0192	118.169	40	< 0.0001 (**)	[2.226; 2.303]
Eyes	Mice Rat	0.022 0.133	116.055	< 0.0001 (*)	0.110	0.0021	52.601	14.165	< 0.0001 (**)	[0.106; 0.115]
Left lung	Mice Rat	0.077 0.464	13.519	0.001 (*)	0.387	0.0097	40.005	14.751	< 0.0001 (**)	[0.367; 0.408]
Right lung	Mice Rat	0.132 0.813	13.546	0.001 (*)	0.681	0.0092	74.362	17.115	< 0.0001 (**)	[0.662; 0.700]
Heart	Mice Rat	0.139 0.720	0.086	0.770	0.582	0.0039	149.742	40	< 0.0001 (**)	[0.574; 0.590]
Liver	Mice Rat	2.045 11.373	0.210	0.649	9.329	0.0091	1029.905	40	< 0.0001 (**)	[9.310; 9.347]
Spleen	Mice Rat	0.113 0.437	0.251	0.619	0.324	0.0062	51.978	40	< 0.0001 (**)	[0.311; 0.336]
Left kidney	Mice Rat	0.196 1.062	6.663	0.014 (*)	0.866	0.0035	244.004	16.679	< 0.0001 (**)	[0.858; 0.873]
Right kidney	Mice Rat	0.246 1.348	14.944	0.0004 (*)	1.102	0.0070	157.667	15.080	< 0.0001 (**)	[1.087; 1.117]
Stomach	Mice Rat	0.282 1.586	0.126	0.725	1.303	0.0037	352.956	40	< 0.0001 (**)	[1.296; 1.311]
Small intestine	Mice Rat	1.507 8.337	0.161	0.691	6.830	0.0037	1850.916	40	< 0.0001 (**)	[6.823; 6.837]
Large intestine	Mice Rat	0.868 4.811	0.155	0.695	3.943	0.0038	1036.818	40	< 0.0001 (**)	[3.935; 3.951]

(*) indicates that variances are unequal ($p < 0.05$); (**) indicates statistical differences highly significant ($p < 0.01$).

Preprints (www.preprints.org) | NOT PEER-REVIEWED | Posted: 27 July 2019 doi:10.20944/preprints201907.0306.v1

Figure 1. Correlation between weights of the pairs organs.

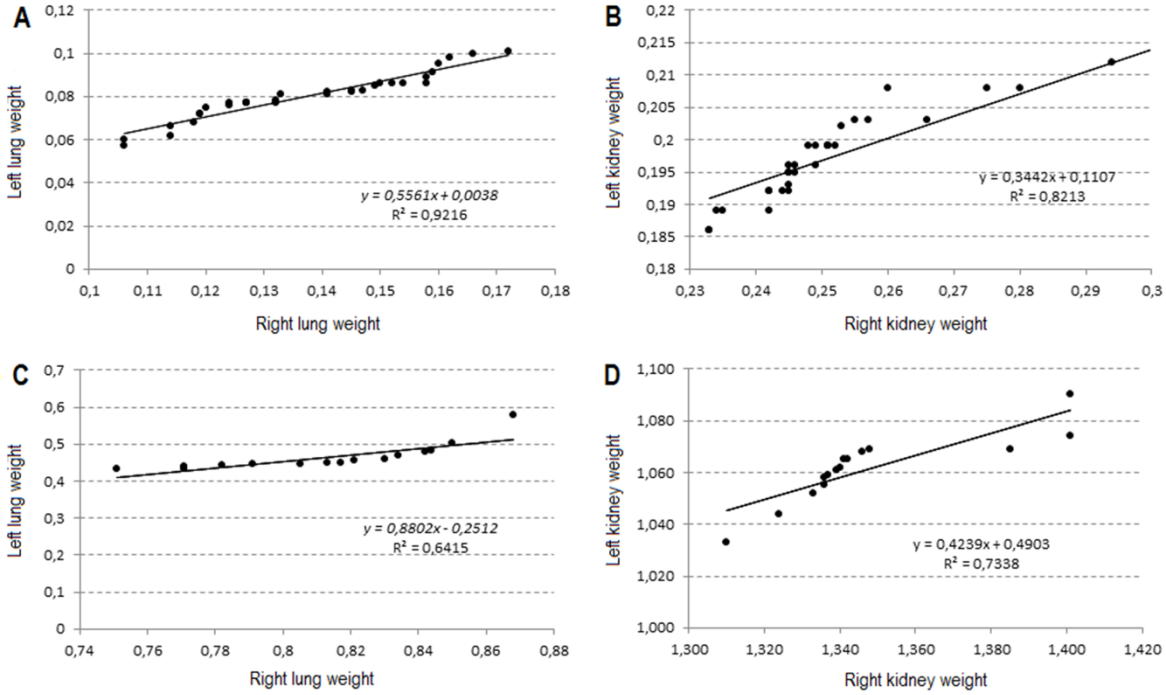

Lungs (right and left) of mice **(A)**; Kidneys (right and left) of mice **(B)**; Lungs (right and left) of rat **(C)**; Kidneys (right and left) of rat **(D)**.

Preprints (www.preprints.org) | NOT PEER-REVIEWED | Posted: 27 July 2019 doi:10.20944/preprints201907.0306.v1

Figure 2. Anatomy and histology of mice and rat brain.

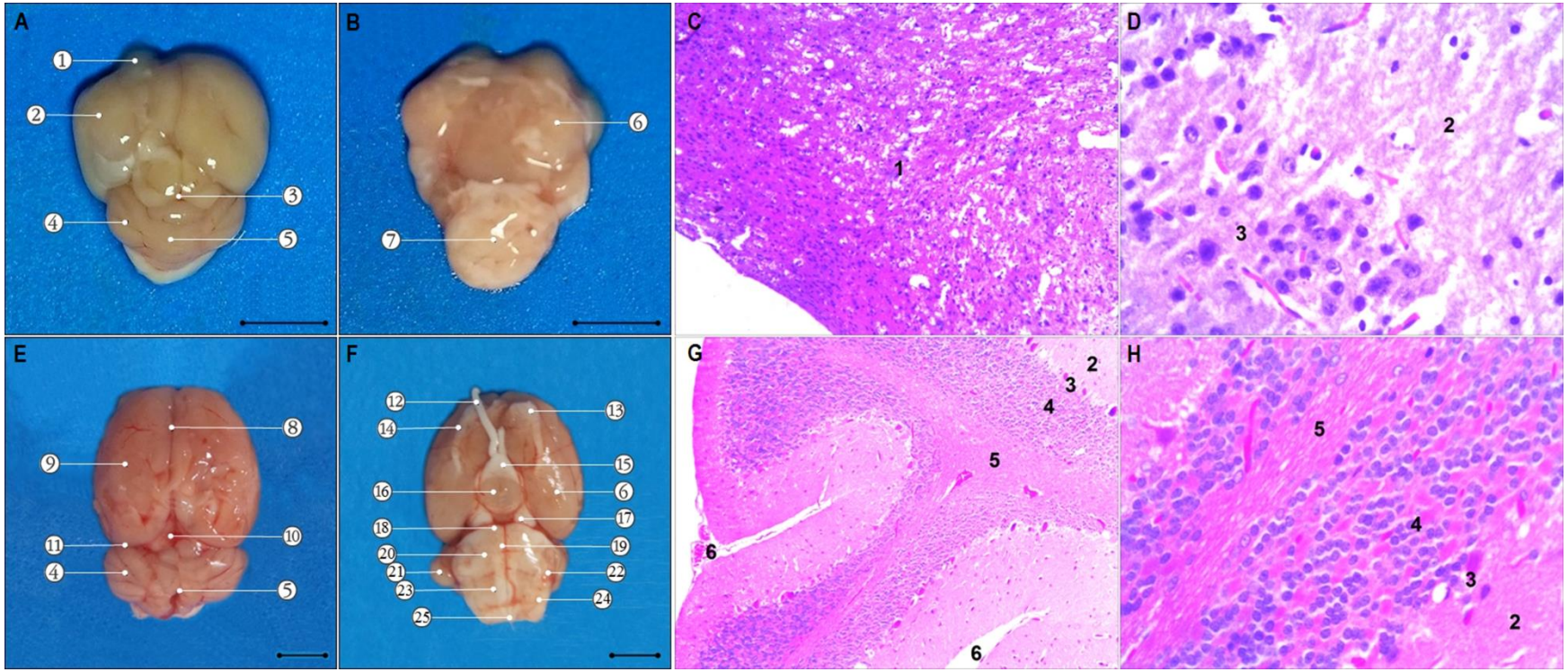

Brain of mice **(A** and **B)** and brain of rat **(E** and **F)** (bar = 5 mm), dorsal surface **(A** e **E)** and ventral surfaces **(B** e **F)** of the cerebral hemispheres: olfactory bulb **(1)**, forebrain (prosencephalon) **(2)**, midbrain (mesencephalon) **(3)**, floculos **(4)**, vermis **(5)**, pyriform cortex **(6)**, romcephalon **(7)**, longitudinal fissure **(8)**, cerebral cortex **(9)**, caudal colliculus **(10)**, transverse fissure **(11)**, optic nerve **(12)**, olfactory bulb **(13)**, lateral olfactory tract **(14)**, optic chiasma **(15)**, mamillary bodies **(16)**, cerebral crus **(17)**, pons **(18)**, ventral medial fissure **(19)**, trapezoid body **(20)**, paraflocculus **(21)**, lateral ventral sulcus **(22)**, medullary pyramid **(23)**, medulla oblongata **(24)** and spinal medulla **(25)**. Mice brain tissue (C e D) 4× and 40× respectively; rat brain tissue **(G** and **H)** 20× and 40× respectively: cerebral cortex **(1)**, molecular layer **(2)**, Purkinje cells **(3)**, granular layer **(4)**, white matter **(5)** and sulcus **(6)**.

Preprints (www.preprints.org) | NOT PEER-REVIEWED | Posted: 27 July 2019 doi:10.20944/preprints201907.0306.v1

Figure 3. Anatomy and histology of mice and rat eyes (right and left).

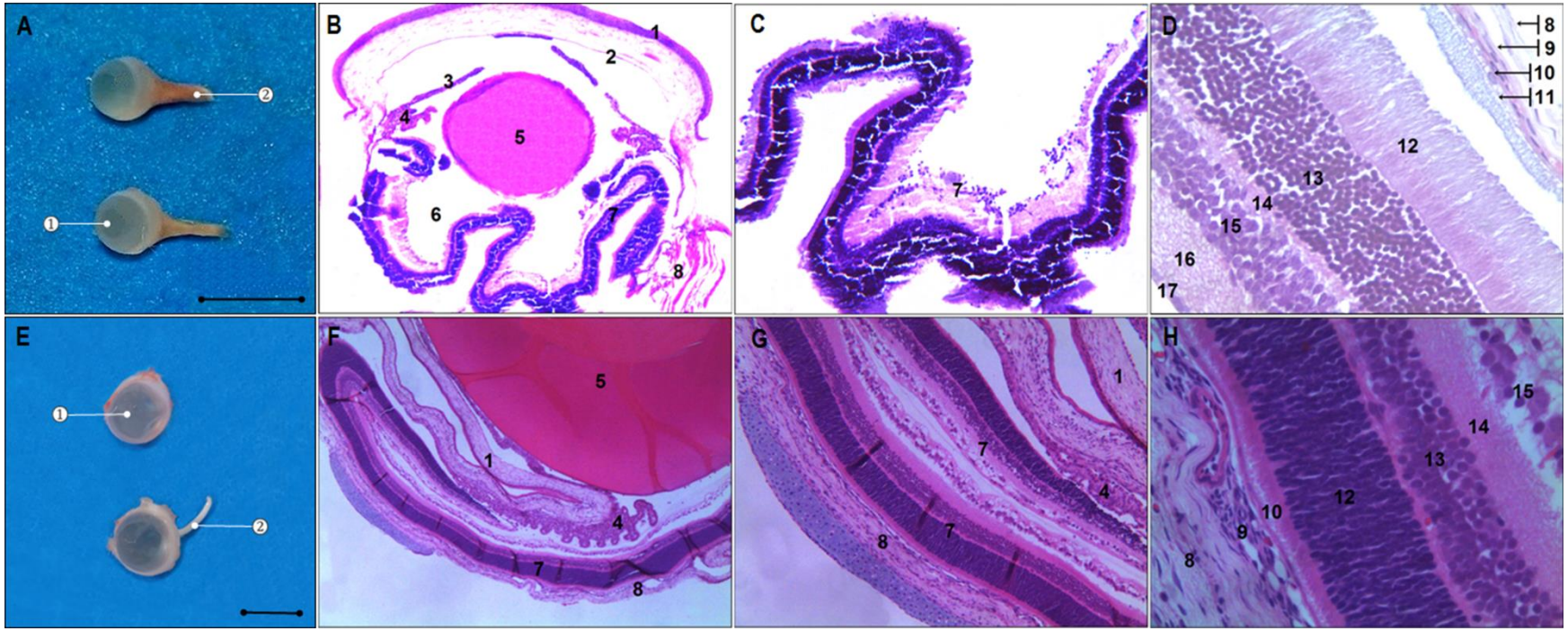

Eyes (right and left) of mice **(A)** and eyes (right and left) of rat **(B)** (bar = 5 mm): eye globe **(1)** and optic nerve **(2)**. Tissues that make up eyes of mice **(B**, **C** and **D)** 4×, 10× and 20× respectively; tissues that make up eyes of rat **(F**, **G** and **H)** 4×, 10× and 40× respectively: cornea **(1)**, anterior chamber **(2)**, iris **(3)**, ciliary body **(4)**, lens **(5)**, vitreous body **(6)**, retina **(7)**, sclera **(8)**, choroid **(9)**, vitreous lamina **(10)**, pigmented epithelium **(11)**, roads and cones **(12)**, outer nuclear layer **(13)**, outer plexiform layer **(14)**, inner nuclear layer **(15)**, inner plexiform layer **(16)** and ganglion cell **(17)**.

Preprints (www.preprints.org) | NOT PEER-REVIEWED | Posted: 27 July 2019 doi:10.20944/preprints201907.0306.v1

Figure 4. Anatomy and histology of mice and rat lungs (right and left).

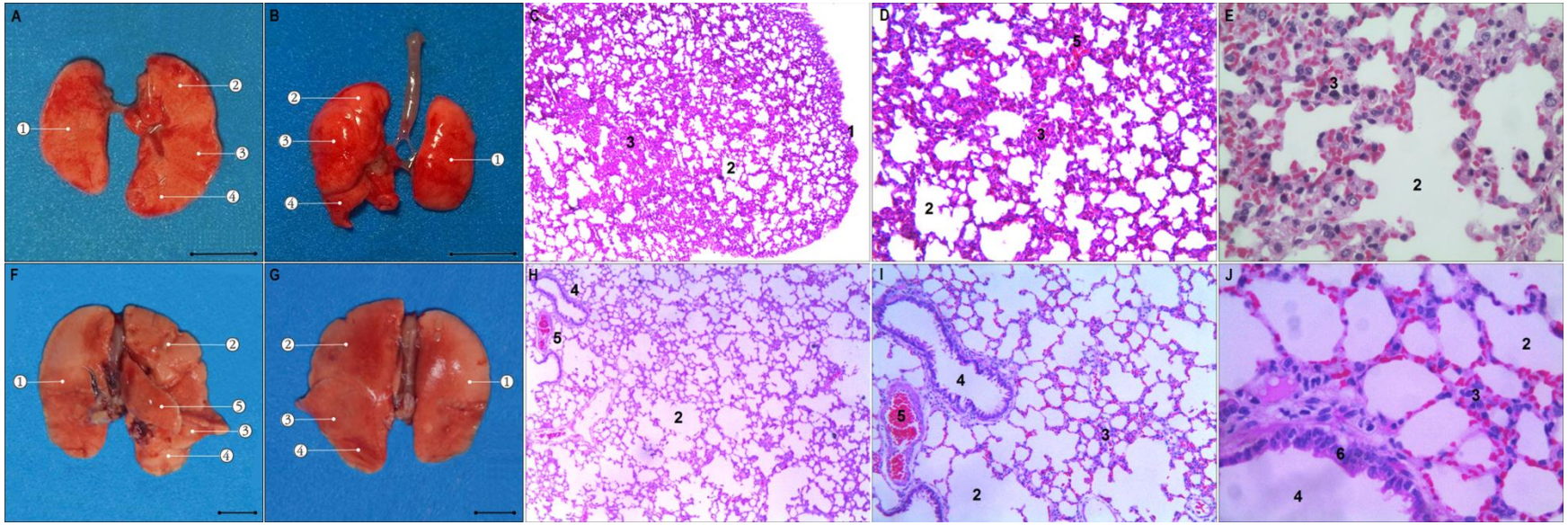

Lungs (right and left) of mice, ventral surface **(A)** and dorsal surface **(B)**; lungs (right and left) of rat, ventral surface **(F)** and dorsal surface **(G)** (bar = 5 mm): left lung **(1)**, right cranial lobe **(2)**, right middle lobe **(3)**, right caudate lobe **(4)** and accessory lobe **(5)**. Pulmonary tissue of mice **(C**, **D** and **E)** 4×, 10× and 20× respectively; pulmonary tissue of rat **(H**, **I** and **J)** 4×, 10× and 20× respectively: pleura **(1)**, alveolus **(2)**, alveolar septum **(3)**, bronchioles **(4)**, pulmonary vein **(5)** and bronchial coating epithelial cells **(6)**.

Preprints (www.preprints.org) | NOT PEER-REVIEWED | Posted: 27 July 2019 doi:10.20944/preprints201907.0306.v1

Figure 5. Anatomy and histology of mice and rat heart.

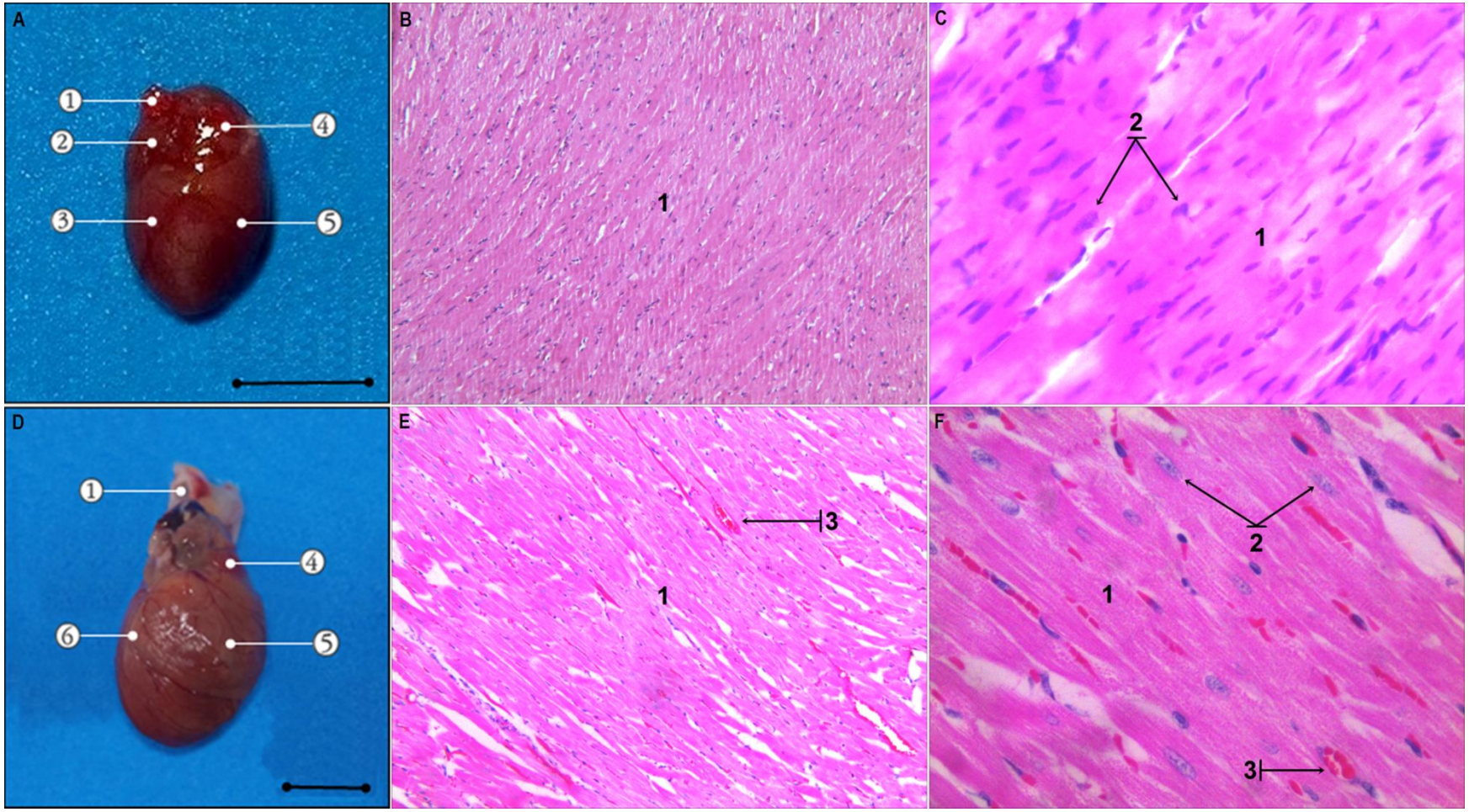

Heart of mice **(A)** and heart of rat **(D)** (bar = 5 mm): aorta **(1)**, left auricle **(2)**, left ventricle **(3)**, right auricle **(4)**, right ventricle **(5)** and conoventricular vein **(6)**. Myocardium of the mice **(B** and **C)** 10× and 40× respectively; myocardium of the rat **(E** and **F)** 10× and 40× respectively: myocardial fibers exhibits cross striations formed by alternation segments **(1)**, myocyte nuclei **(2)** and vein **(3)**.

Preprints (www.preprints.org) | NOT PEER-REVIEWED | Posted: 27 July 2019 doi:10.20944/preprints201907.0306.v1

Figure 6. Anatomy and histology of mice and rat liver.

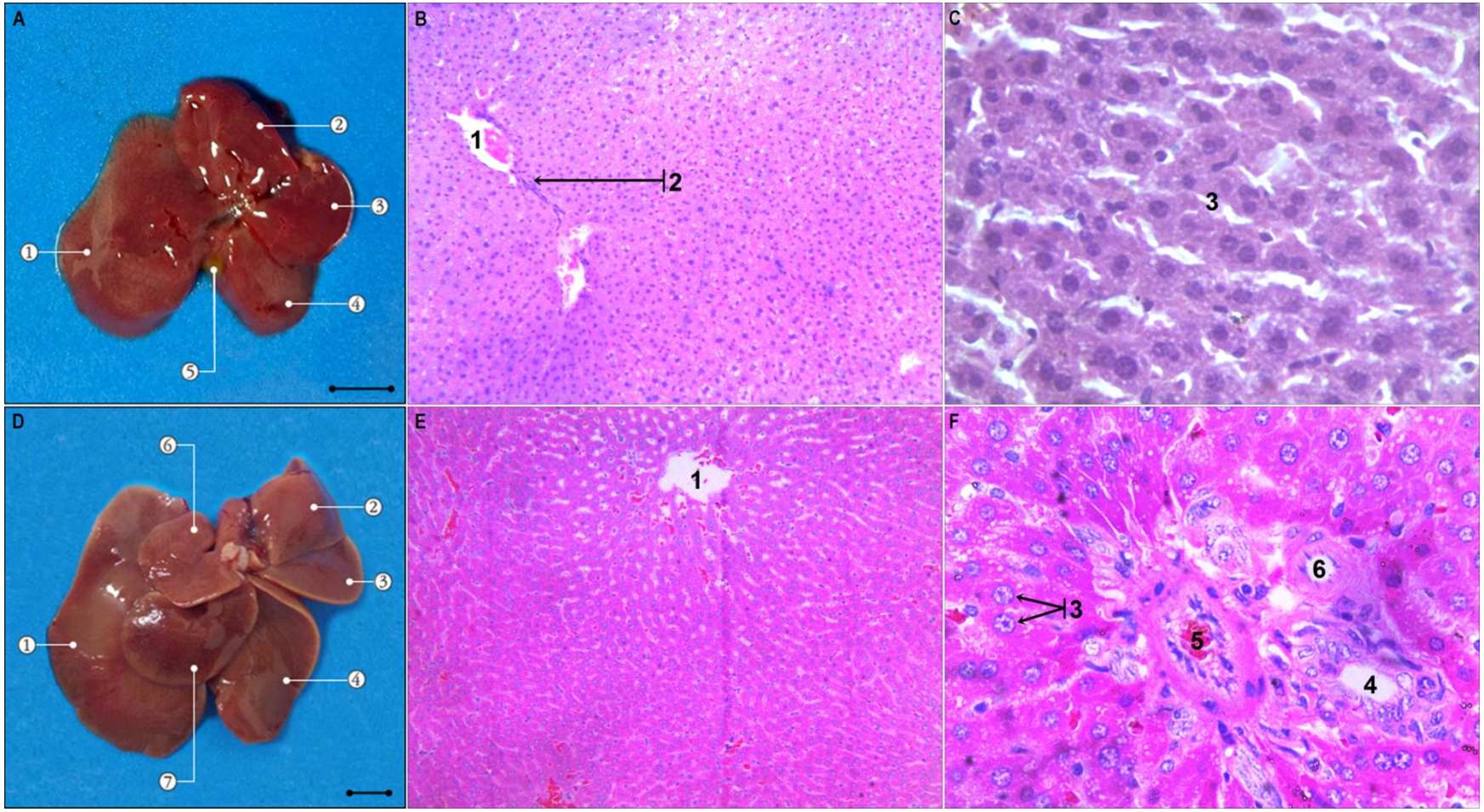

Visceral surface of liver mice **(A)** and visceral surface of liver rat **(D)** (bar = 5 mm): left lateral lobe **(1)**, caudate lobe **(2)**, right lateral lobe **(3)**, right middle lobe **(4)**, gallbladder **(5)**, papillary process **(6)** and left middle lobe **(7)**. Hepatic tissue of mice **(B** and **C)** 10× and 20× respectively; hepatic tissue of rat **(E** and **F)** 10× and 40× respectively: central vein **(1)**, sinusoid **(2)**, hepatocyte **(3)**, portal triad: portal vein **(4)**, hepatic artery **(5)** and bile duct **(6)**.

 doi:10.20944/preprints201907.0306.v1

Figure 7. Anatomy and histology of mice and rat spleen.

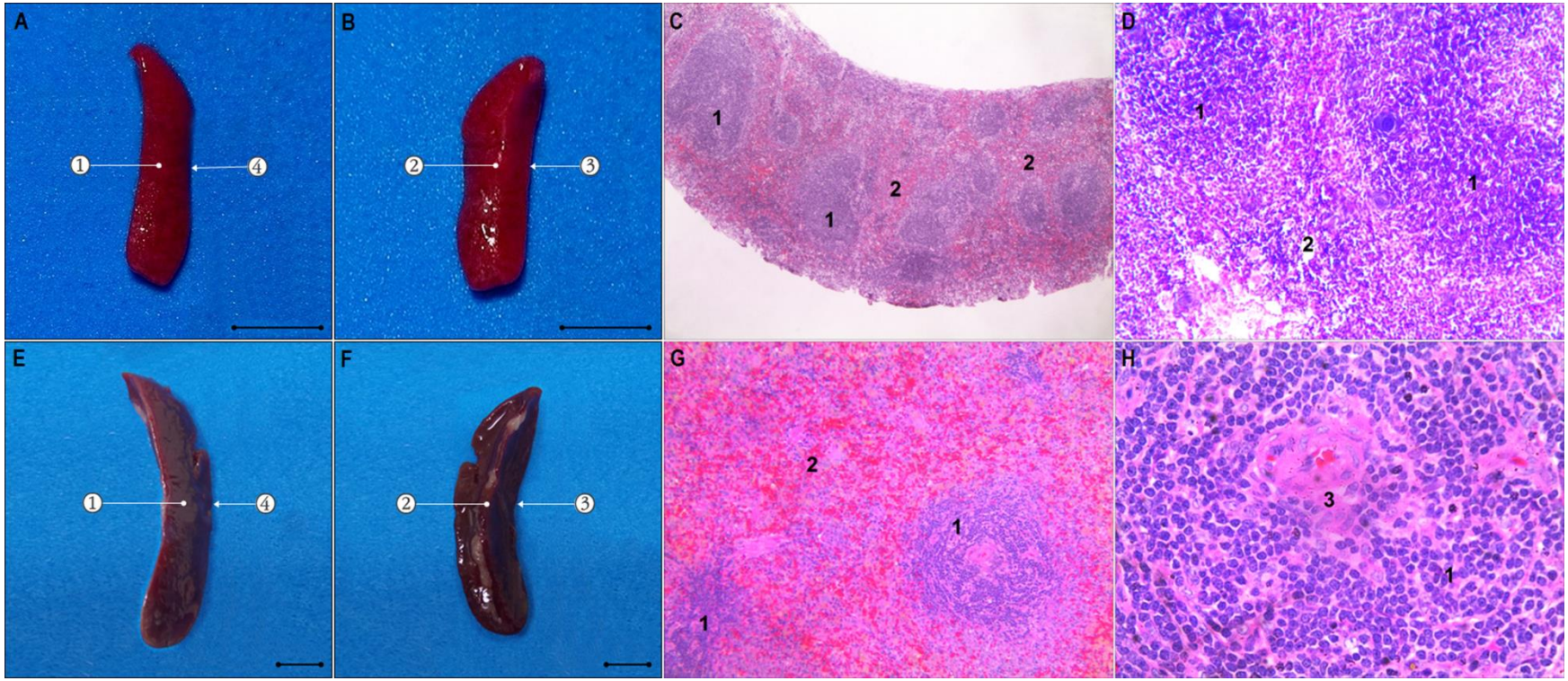

Spleen of mice **(A** and **B)** and spleen of rat **(E** and **F)** (bar = 5 mm): colic surface **(1)**, gastric surface **(2)**, diaphragmatic surface **(3)** and renal surface **(4)**. Splenic tissue of mice **(C** and **D)** 4× and 20× respectively; splenic tissue of rat **(G** and **H)** 20× and 40× respectively: white pulp **(1)**, red pulp **(2)** and central artery **(3)**.

Preprints (www.preprints.org) | NOT PEER-REVIEWED | Posted: 27 July 2019 doi:10.20944/preprints201907.0306.v1

Figure 8. Anatomy and histology of mice and rat kidneys (right and left).

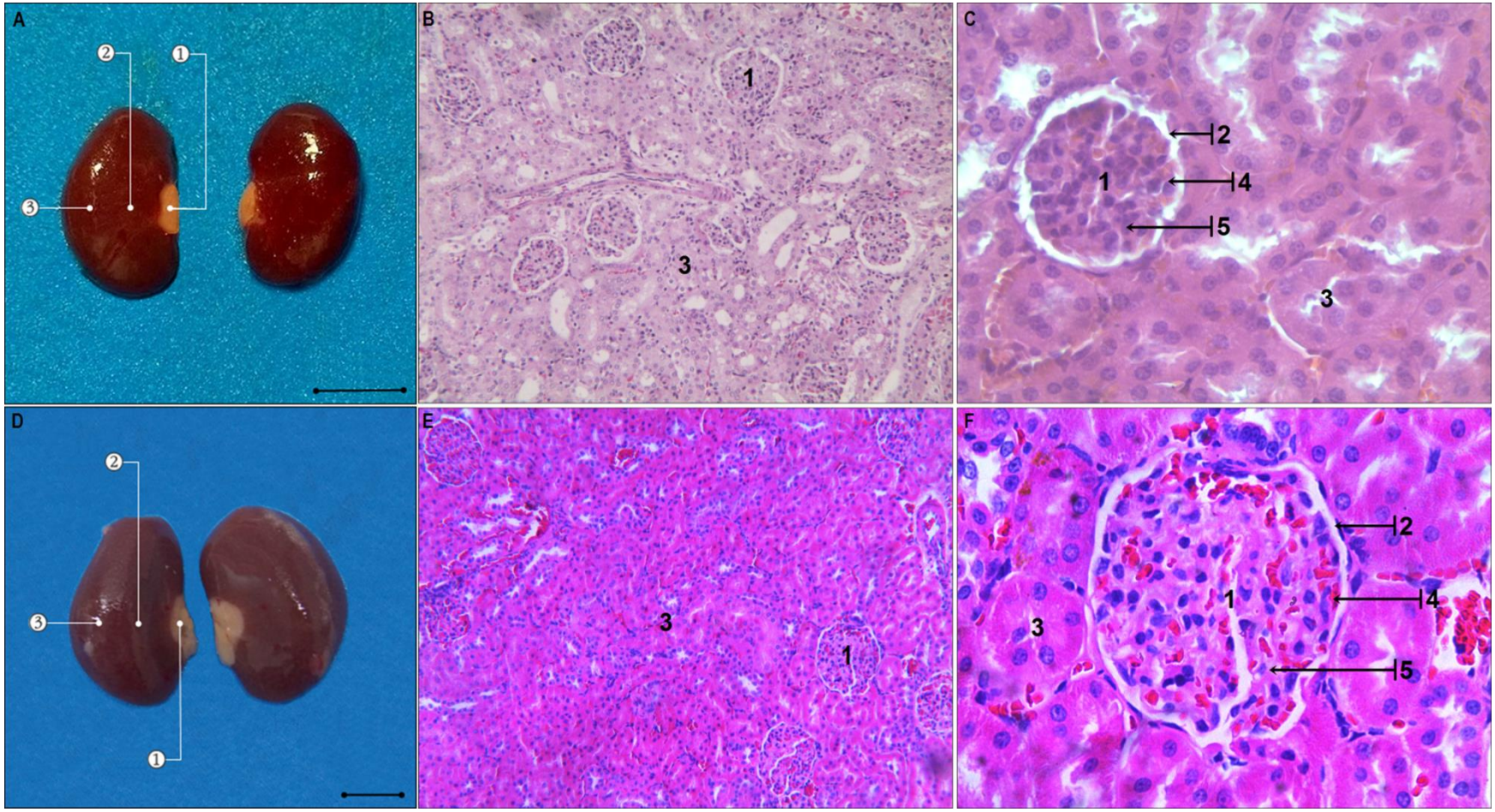

Kidneys (right and left) of mice **(A)** and kidneys (right and left) of rat **(D)** (bar = 5 mm): papilla **(1)**, medulla **(2)** and cortex **(3)**. Renal cortex of mice **(B** and **C)** 10× and 20× respectively; Renal cortex of rat **(E** and **F)** 10× and 40× respectively: glomerulus **(1)**, Bowman's space **(2)**, renal tubules **(3)**; capillary **(4)** and mesentery **(5)**.

Preprints (www.preprints.org) | NOT PEER-REVIEWED | Posted: 27 July 2019 doi:10.20944/preprints201907.0306.v1

Figure 9. Anatomy and histology of mice and rat stomach and small intestine.

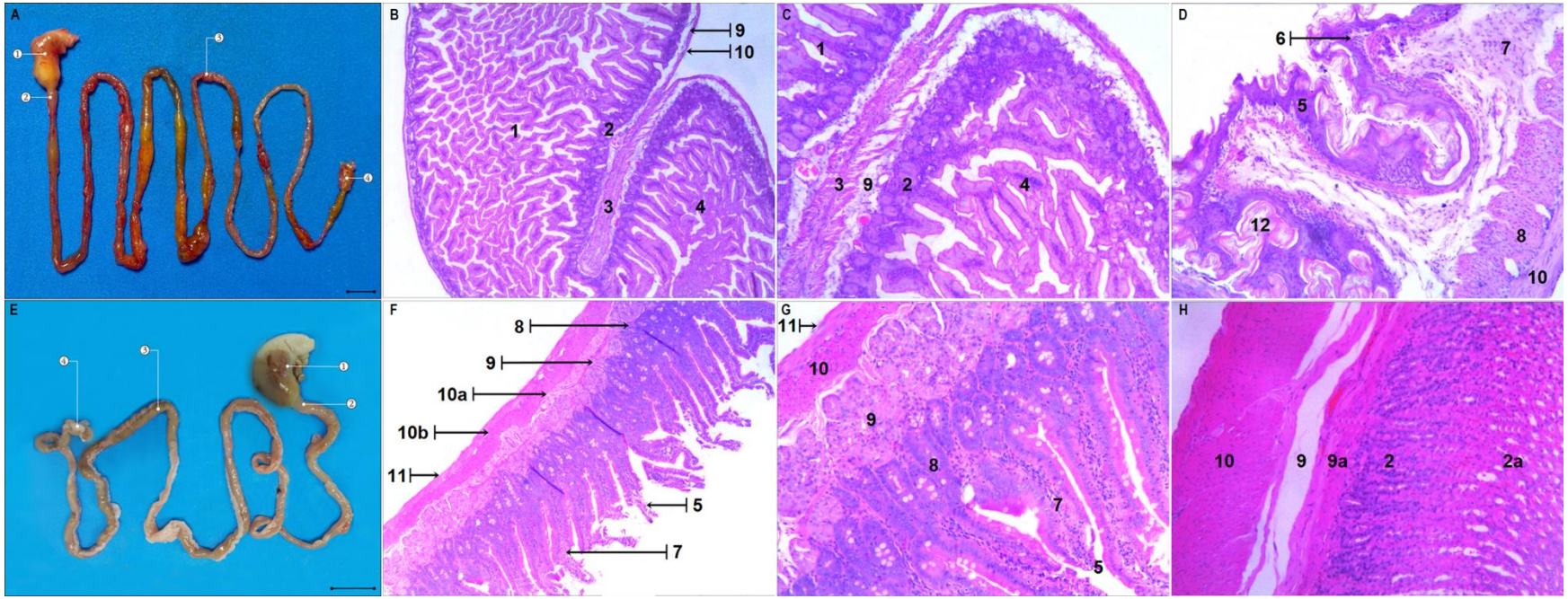

Stomach and small intestine of mice **(A)** and stomach and small intestine of rat **(E)** (bar = 5 mm): stomach **(1)**, duodenum **(2)**, jejunum **(3)** and ileus **(4)**. Stomach of mice **(B**, **C** and **D)** 4×, 10× and 40× respectively; jejunum of rat **(F**, **G** and **H)** 4×, 10× and 40× respectively: mucosa of the aglandular stomach **(1)**, main cells **(2)**, parietal cells **(2a)**, limiting crest **(3)**, mucosa of the glandular stomach **(4)**, villi **(5)**, absorbent columnar cells **(6)**, lamina propria **(7)**, crypts **(8)**, submucosa **(9)**, muscularis mucosae **(9a)**, layer muscular **(10)**, internal circular muscular layer **(10a)**, outer longitudinal muscular layer **(10b)**, adventitia **(11)** and cardiac gland **(12)**.

Preprints (www.preprints.org) | NOT PEER-REVIEWED | Posted: 27 July 2019 doi:10.20944/preprints201907.0306.v1

Figure 10. Anatomy and histology of mice and rat large intestine.

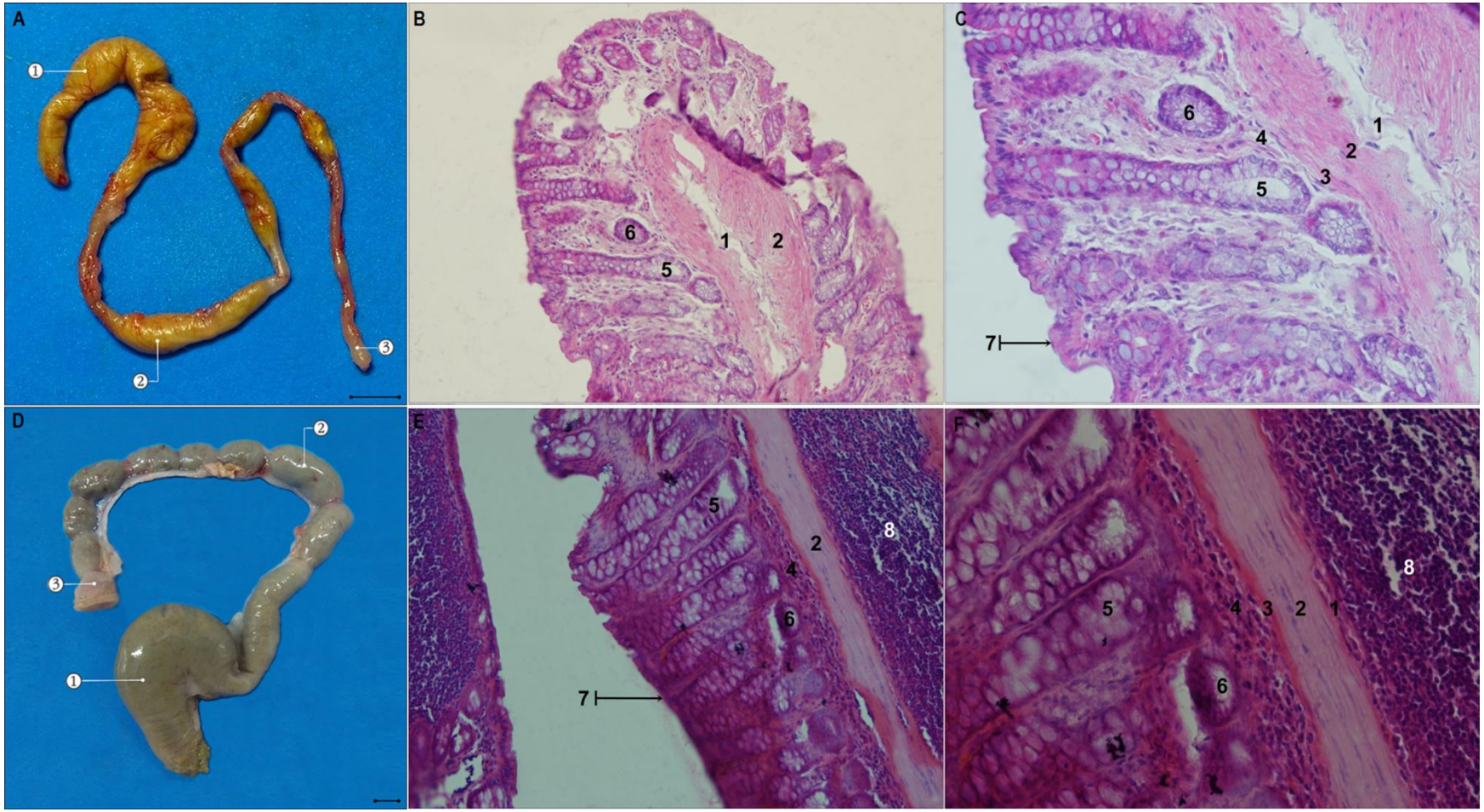

Large intestine of mice **(A)** and large intestine of rat **(B)** (bar = 5 mm): cecum **(1)**, colon **(2)** and rectum **(3)**. Cecum of rat **(B** and **C)** 10× and 40× respectively; colon of rat **(E** and **F)** 10× and 40× respectively: serosa (visceral peritoneum) **(1)**, muscular layer **(2)**, fine submucosa **(3)**, submucosa **(4)**, crypt elongation **(5)**, Lieberkühn's glands **(6)**, goblet cells **(7)** and lymphatic follicle **(8)**.